Received: 9 November 2020 | Revised: 17 May 2021 | Accepted: 20 June 2021

DOI: 10.1002/eco.2321

RESEARCH ARTICLE

WILEY

Green roof vegetation management alters potential for water quality and temperature mitigation

Valerie Ouellet[1] | Kieran Khamis[1] | Danny Croghan[1] | Liliane M. Hernandez Gonzalez[2] | Viviane A. Rivera[2] | Collin B. Phillips[3] | Aaron I. Packman[2] | William M. Miller[2] | Richard G. Hawke[4] | David M. Hannah[1] | Stefan Krause[1,5]

[1]School of Geography, Earth and Environmental Sciences, and Institute for Global Innovation, University of Birmingham, Birmingham, UK

[2]McCormick School of Engineering, Northwestern University, Evanston, Illinois, USA

[3]Civil and Environmental Engineering Department, Utah State University, Logan, Utah, USA

[4]Chicago Botanic Garden, Glencoe, Illinois, USA

[5]Univ Lyon, Université Claude Bernard Lyon 1, CNRS, ENTPE, UMR5023, Ecologie des Hydrosystèmes Naturels et Anthropisés (LEHNA), Villeurbanne, France

Correspondence
V. Ouellet, School of Geography, Earth and Environmental Sciences, and Institute for Global Innovation, University of Birmingham, Birmingham B15 2TT, UK.
Email: valeria.ouellet@gmail.com

Funding information
U.S. National Science Foundation, Grant/Award Number: CBET-1848683; European Union's Horizon 2020 Research and Innovation Programme under the Marie Sklodowska-Curie, Grant/Award Number: 34317

Abstract

The global increase of urban impervious land cover poses a significant threat to the integrity of river ecosystems. Hence, it is critical to assess the efficiency of green roofs (GR) to mitigate the negative impacts of urbanization on river ecosystems, such as thermal surges and pollutants. In this study, we evaluated the eco-hydrological behaviour of two fully established GR under differing management regimes at the Chicago Botanical Gardens from July to September 2019. The drainage outflow from a non-vegetated roof, a managed GR (perennial native and non-native plants) and an unmanaged GR (perennial natural prairie vegetation) were monitored, and thermal dynamics, dissolved organic matter (DOM) composition and nitrate concentration assessed. The managed GR runoff had a lower DOC concentration and less humic-like DOM signal ($SUVA_{254}$) compared to the unmanaged GR. In contrast, lower concentrations of nitrate and more recalcitrant DOM (less protein-like compounds relative to humic-like compounds) were associated with the unmanaged GR. The unmanaged GR also displayed a greater capacity to reduce thermal surges associated with storm events. Our study provides new information on the implications of GR management for water quality with particular relevance to the urban stream syndrome. Further, the impacts of GR management on the mitigation of thermal surges and DOM composition can help to improve future GR design, as these ecohydrological responses have been largely overlooked to date. Our findings can support future urban planning, particularly for scenarios where green infrastructures are used to mitigate the impacts of climate change on urban river ecosystems.

KEYWORDS
cities, DOM, green roof, mitigation, nitrate, thermal surges, urbanization

V. Ouellet and K. Khamis contributed equally to this research and shared co-first authorship.

1 | INTRODUCTION

The UN 2019 Revision of World Population report (United Nations, 2019) states that 55% of the world's population lives in urban areas, a proportion that is expected to increase to 68% by 2050, with more than 43 megacities exceeding 10 million inhabitants by 2030 (D'Amour et al., 2017; Shafique et al., 2018). Consequently, urban areas are forecast to triple by 2030 compared to 2000. Most of the world's population will be impacted by climate change in urban areas, with climate extremes causing more frequent and severe flooding and heatwaves (Seto et al., 2012; Ward et al., 2016). For example, summer heatwaves are responsible for millions of deaths worldwide yearly, and excess mortality is projected to increase in the future (Guo et al., 2018). Heatwaves also enhance the intensity of urban heat island effects (UHI), which can significantly increase the heat stress in cities (Deilami et al., 2018; Timm et al., 2020) by inducing an increase in air temperatures up to 15°C (Mohajerani et al., 2017; Santamouris, 2014). Due to positive feedback interaction between heatwaves and UHI, urban areas can experience elevated heat stress, which has become a major concern due to not only the impacts on human health but also on power grids and infrastructure (He et al., 2020).

Urban planners and engineers are now assessing mitigation strategies to decrease flood risk and UHI, both of which are associated with greater proportions of impervious surfaces. As roofs typically represent around 32% of the horizontal surface of built-up areas (Frazer, 2005), vegetated roofs (so-called green roofs [GR]) have become a popular mitigation strategy to offset several negative impacts that urban land cover has on aquatic ecosystems (Berndtsson, 2010; Mentens et al., 2006; Shafique et al., 2018). With many countries providing incentives, GR surfaces have significantly increased over the last 15 years (up to 8 km^2/year) in numerous cities across North America and Europe (Cascone et al., 2018; Shafique et al., 2018). GR have been shown to reduce runoff, minimize pollutant discharge, decrease erosion and maintain base flows of receiving streams (Cipolla et al., 2016; Loiola et al., 2019; Zhang et al., 2019).

Beyond the UHI and runoff extremes (e.g. peak and total volume), thermal pollution is an often neglected but important consequence of heat exchange and hydrological process alterations associated with urbanization (Timm et al., 2020). Storm runoff can result in summer thermal surges in aquatic ecosystems, reaching up to 7°C and sometimes lasting for several hours (Croghan et al., 2019; Nelson & Palmer, 2007). Urban streams generally display warmer thermal regimes overall (Ketabchy et al., 2018; Somers et al., 2013). Therefore, mitigating the thermal impacts of urban expansion has become both a research and planning priority over the last few decades (Coker et al., 2018; Hu et al., 2019; Pour et al., 2020; Sohn et al., 2017). However, the thermal behaviour of GR runoff has yet to be characterized.

GR can also alter the flux of nutrients and dissolved organic carbon (DOC) from the roof to the receiving drainage network relative to un-vegetated roofs. GR alter nitrogen cycling with the potential to either reduce or increase the concentration of inorganic nitrogen fluxes (NO_3, NH_4) relative to un-vegetated roofs (Dusza et al., 2017; Seidl et al., 2013). Regarding DOC, GR generally lead to an increase in DOC concentration (often in excess of 30 mg/L), with hydrological export representing an important component of the roof carbon budget (Buffam & Mitchell, 2015). The potential for storage and processing of carbon is largely a function of substrate type and depth. For example, biochar can be used to reduce DOC export (Beck et al., 2011). Information regarding the impact of GR vegetation cover and management on dissolved organic matter (DOM) composition remains limited, despite the effects that highly humic (recalcitrant DOM) or highly labile DOM loadings can have on receiving waters (Ritson et al., 2014).

In the last few decades, more studies have focused on the ecological aspects of GR, such as community dynamics (plants, insects and microbial communities) or their agricultural potential. They have highlighted the numerous ecosystem services that GR can provide, such as biodiversity/pollination enhancement, building thermal protection and human well-being (Hoch et al., 2019; Lata et al., 2018; Thuring & Dunnett, 2019). However, GR remain primarily treated as an engineering or horticultural challenge, rather than as ecological systems. This focus has influenced their physical layout and vegetation composition, which is heavily controlled by the structural constraints of buildings (Cascone et al., 2018). GR management, meaning the type of vegetation used and routine maintenance (irrigation, fertilization, substrate renewal, etc.), plays a significant role in the GR water retention capacity. Indeed, the water holding capacity and evapotranspiration process can vary between species and are primary controls over water retention (Dunnett et al., 2008; Nagase & Dunnett, 2012). This capacity is modulated by the depth and composition of the soil layer and the roof slope (Berndtsson et al., 2006; Hashemi et al., 2015). Therefore, the magnitude and direction of change in the runoff composition are related to multiple factors, including plant composition (species-specific release of N from root and leaf exudates that can offset uptake), substrate depth (first-order control on moisture, temperature, microbial habitat and binding/exchange sites) and management interventions such as application of fertilizers (Buffam & Mitchell, 2015).

Although the influence of GR on water quality parameters has been previously studied, few studies have comprehensively evaluated the effects of different vegetation management regimes on runoff temperature, nutrients and DOM quality (Buffam et al., 2016; Whittinghill et al., 2016). Therefore, it is difficult to holistically assess the performance of GR and support the design of more efficient GR that goes beyond the hydrological benefits. Additionally, the existing knowledge is biased towards small experimental plots at relatively short timescales and mainly on newly installed GR (Beecham & Razzaghmanesh, 2015; Liu, Wei, et al., 2019). It is thus challenging to upscale GR water quality dynamics to the roof scale, particularly in responses to variability with regard to discrete storm events and the effect of antecedent conditions.

Given the research gaps outlined above, the aim of this study was to investigate the efficiency of two semi-intensive established GR to mitigate the impacts of urbanization on water quality (i.e. DOM quality and quantity and nitrate) and thermal surges associated with

stormwater runoff. In particular, we wanted to improve understanding of how differing GR structures (e.g. vegetation and management) impact their utility as mitigation tools in urban areas by (1) quantifying the water quality responses for multiple different storm events over 2 months during the summer of 2019 and (2) identifying the drivers and controls of the observed responses. The information gained from this study will help to improve our understanding of key processes that can used to guide urban planning and help improve GR design.

2 | METHODS

2.1 | Study area and monitoring setup

We studied two semi-intensive GR and an adjacent non-vegetated roof from July to September 2019. All three roofs were located on The Daniel F. and Ada L. Rice Plant Conservation Science Center at the Chicago Botanic Garden, Illinois, USA (42.14°N, −87.78°E), and were purpose-built in 2009 as part of the original building design (Figure 1). The North GR featured perennial native and non-native plants, as well as a variety of sedums (*Sedum* spp.) planted in three linear ribbons that bisect the roof from east to west (hereafter referred to as the managed GR). In contrast, the South GR (herein referred to as the unmanaged GR) was planted with perennial native plants that are representative of a natural prairie in the Midwest United States (Figure 2; Hawke, 2015). For both GR, the growing medium consisted of a mixture of expanded clay and shale, vermiculite, perlite, sand and organic matter. There was no fertilization of the roofs, and artificial irrigation (water) was only provided on a limited basis during periods of extreme drought, which did not occur during our study. The drainage panel on each roof drained 743 m^2 and channelled water to the central roof drain that empties into a bioswale surrounding the building. The non-vegetated part of the roof consisted of concrete with a 93-m^2 drainage area and was used as a baseline for evaluating the managed and unmanaged GR.

As shown in Figure 1, each GR roof section was constructed with the following sensors embedded in the roof: air temperature (°C), soil moisture (saturation in %) soil temperature (°C). A standard meteorological station was also present on the building, providing air temperature (°C), solar radiation (W/m^2) and wind speed (m/s). Precipitation data (mm) were extracted from a weather station situated 6.6 km from the Botanic Garden (NOAA's climate data online; NOAA, 2020). We equipped the drain of each roof section with water temperature (°C; HOBO MX2203 loggers) and discharge (m^3/s) sensors and a bespoke small-footprint auto-sampler to collect samples for the water quality analysis (Table 1 and Figure S1).

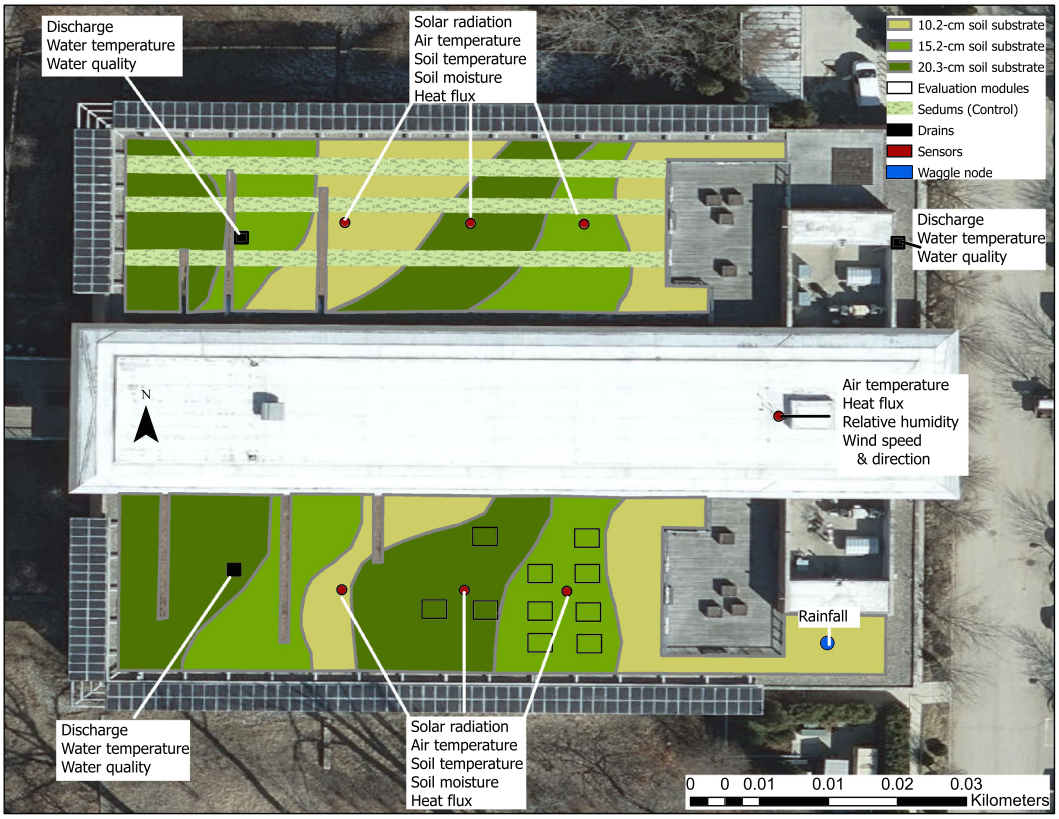

FIGURE 1 Schematic diagram of the green roofs with sensors, drains, vegetation and substrate depths highlighted superimposed on an aerial photograph

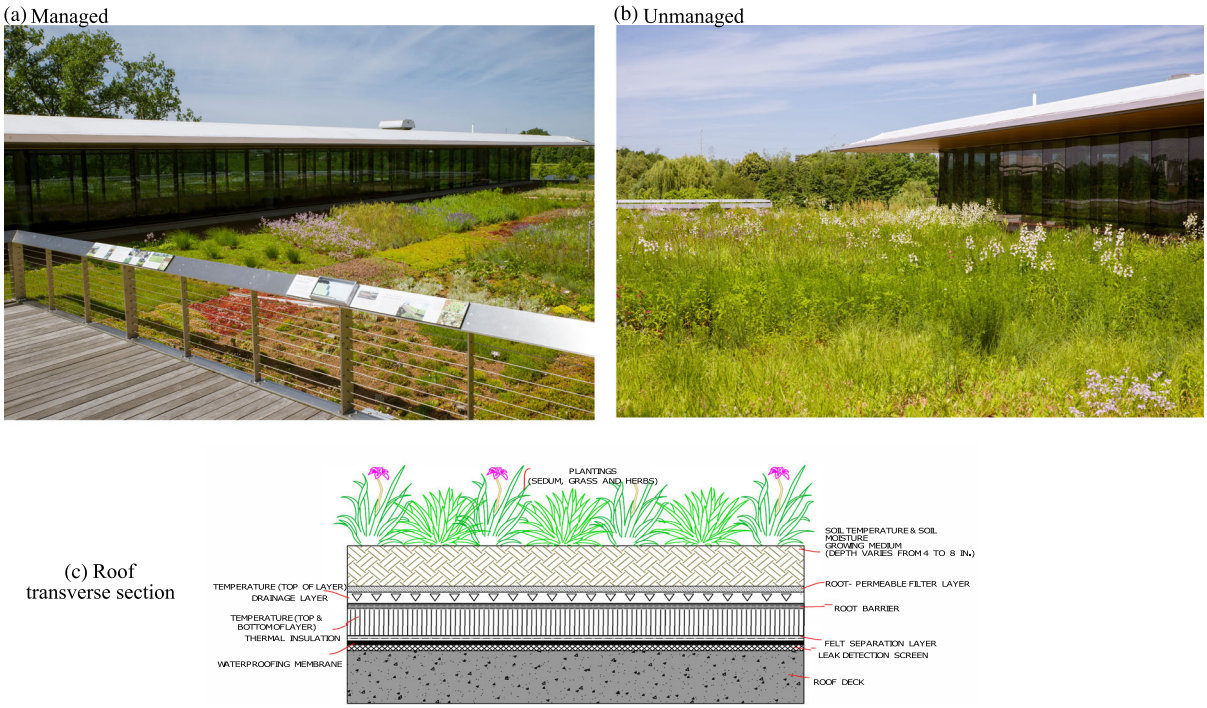

FIGURE 2 Photographs from (a) managed GR planted with native and non-native plants in three ribbons and (b) unmanaged GR planted with regional native prairie plants. (c) A schematic of the roof layer design (identical for both GR) (images extracted from Hawke, 2015)

TABLE 1 Variables monitored, including resolution and instrumentation used

Variable	Monitoring resolution (minute)	Location	Instrumentation and method of collection
Meteorological variables (air temperature [°C], relative humidity [%] and wind speed [m/s])	15	Green roof	107 temperature probe, HMP50-L temperature and relative humidity probe and 85000 ultrasonic anemometer equipped with Campbell Scientific data loggers
Flow discharge[a] (m^3/s)	5	Drains indicated in Figure 1	Stingray 2.0 area velocity flowmeter installed within drains under green roof
Water quality variables (DOC, DOM quality, major anions)	Variable— – initial 5 min, longer duration during recession	Drains indicated in Figure 1	Bespoke small-volume autosamplers installed under the roof, collecting from sample basin
Drainage water temperature (°C)	1	Drains indicated in Figure 1	HOBO MX2203 loggers installed directly into drainage pipe for all drains

[a]Flow controls were required to instal the sensors, and the resulting measurement sensitivity was not sufficient to reliably capture runoff over the full range of hydrological conditions. The data were not used for the subsequent analysis.

2.2 | Water quality

To assess the water quality response associated with each roof type, we measured temperature, DOM (quality and quantity) and nutrient dynamics. We looked at the initial response (hereafter called first flush) of the roof to a rainfall event (observations recorded during the first 15 min of each event) to capture the higher mass associated with runoff during the onset of events (Berndtsson et al., 2008). Water samples were collected using a custom autosampler for small-volume sample collection. Sampling locations are shown in Figure 1. The device was built using low-cost components and consisted of a peristaltic pump, stepper motor, microcontroller (including associated electronic components for driving motors and timekeeping), suction hose and sample tube holder (Figure S1). These components were

housed in a waterproof case initially designed for camera equipment. This device was chosen in preference to a larger commercial autosampler, due to ease of transport, the size (needed to fit under a building) and the water volume collected sufficient for our analyses. The autosampler was triggered by a float switch situated at the exit of the discharge drain, where it collected 14 × 50 mL samples at a defined time step. The minimum flow required to initiate sampling was 0.01 m^3/s. This threshold was defined to ensure we capture rainfall events that were big enough to initiate DOM and nutrient transport. Water samples were collected from autosamplers within 24 h and filtered immediately after collection using 0.20-μm nylon membrane filters. Samples were then stored in a refrigerator until analysed. Sensitive samples (e.g. DOC) were analysed within 24 h of collection.

DOC was determined using a Tekmar Dohrmann Apollo 9000 Total Organic Carbon (TOC) combustion analyser. For each sample, replicate DOC readings ($n = 3–5$) were undertaken, and ≤2% coefficient of variation was observed. Absorbance spectra (200–850 nm) were measured using a Shimadzu UV-2450 UV-Vis spectrophotometer (cuvette path length 10 mm) with quartz cuvettes that were triple rinsed with sample water. A QuantaMaster 40 UV-VIS spectrofluorometer was used to measure fluorescence. Step size for the measurements was set at 1 nm, with an integration time of 0.5 s, with results averaged over three measurements. A blank was measured at the start of each instrument run to calibrate fluorescence intensity (Lawaetz & Stedmon, 2009). Excitation (1 nm slit width) and emission (2 nm slit width) were determined for each sample for wavelength pairs corresponding to Peak T (tryptophan-like: fluorescence related to amino acids and free or bound in proteins, Ex. 270 nm, Em. 304 nm), Peak C (humic-like: fluorescence related to high molecular weight humic compounds, Ex. 350 nm, Em. 420–480 nm), humification index (Ex. 254 nm, Em. 435–480 nm), fluorescence index (Ex. 370 nm, Em. 450–500 nm) and biological index (Ex. 310, Em. 380–435). $SUVA_{254}$, an index of carbon aromaticity (Weishaar et al., 2003), was calculated as the absorption coefficient at 254 nm divided by DOC concentration. Fluorescence Peak C, Peak T and the ratio (C:T) was used to provide an indication of recalcitrant to labile DOM (Baker, 2001). Fluorescence-based indices of DOM humification (HI), DOM freshness (FI) and biological activity (BI) were calculated following Hansen et al. (2016). To provide an indication of DOM molecular weight, spectral slopes at 275–295 nm (SS_{275}), 350–400 nm (SS_{350}) and their ratio (SR) were also calculated (Helms et al., 2008). Nitrate and phosphate were analysed using an 881 Compact Ion Chromatography pro instrument, and electrical conductivity was measured using the conductivity meter ES-12.

2.3 | Metrics and statistical analysis

During the monitoring period, 15 discrete storm events were observed above the measurement threshold (SI; Table S1); however, due to equipment failure, water temperature data were obtained for only 12 events, and water chemistry data were obtained for 11 events.

To better understand the behaviour of the roofs, we calculated a suite of metrics to characterize storm event response, antecedent conditions and thermal response.

- The storm event characteristics included the maximum hourly rainfall intensity (P_{int} mm/h) and total rainfall (P_{tot} mm).
- The antecedent conditions of the roof were defined by the total rainfall (mm) before the specific storm (P_{3D} and P_{5D}, 3- and 5-day sums, respectively), the magnitude of the most recent previous event (M_{prev}), the time since the previous event (T_{prev} minutes), the potential evapotranspiration (PE_{3D} and PE_{5D}) calculated using the Penman–Monteith equation (cumulative over 3 and 5 days), the aridity index ($Arid_{3D}$ and $Arid_{5D}$, 3- and 5-day sums, respectively) and the moving average air temperature (AT_{3D} and AT_{5D} °C, 3 and 5 days).
- The thermal behaviour (°C) of the roof was characterized by the maximum (MaxT), the minimum (MinT) and the mean (MeanT) temperature during the event, as well as the temperature differences (TempD) between the start and end of the event (pulse/surge), the time to reach maximum/minimum values (Start time − TimeMax/TimeMin in minutes) and the variance of each event (Var).

The GR design and history of plant research on these roofs provided us with a unique opportunity to assess stormwater runoff from distinct roof growing media and plant communities in a single locality (i.e. building). In particular, it enabled us to assess responses to identical meteorological histories, including precipitation and antecedent, conditions that could not be achieved elsewhere. However, this meant that our study was pseudoreplicated, which was a consequence of working at the whole roof scale, while having identical meteorological inputs across all roofs. There is currently debate in the ecological literature regarding the best way to deal with pseudoreplication as it is inherent to many larger scale designs (Colegrave & Ruxton, 2018; Davies & Gray, 2015). In this case, we have undertaken statistical analysis to reduce the impact of pseudoreplication, but the confirmatory analysis should be interpreted with this in mind. Principal component analysis (PCA) was undertaken using the *FactoMineR* package (Husson et al., 2014) to identify variables that explained the most variance across storms. Also, to further explore DOM quality dynamics, we used ordination (PCA) to reduce the absorbance and fluorescence metrics outlined above into two axes. Variable correlation scores for the PCA axes were also used to reduce the number of metrics used in statistical analysis and avoid inducing bias due to collinearity between variables (SI; Table S2 and Figure S2). The metrics retained for further analysis were P_{tot}, P_{int}, T_{prev} and M_{prev}, antecedent air temperatures (AT 3–5 days) and antecedent evapotranspiration potential (PE 3–5 days). Based on the literature and the anticipated differences between roof types, we selected a core suite of response variables that characterized important characteristics of roof function and runoff: bulk solute concentration (quantified as electrical conductivity), dissolved carbon quantity

(total DOC), nitrogen efflux (nitrate), DOM aromaticity (SUVA) and molecular weight (spectral slope ratio SR) and thermal surge (water temperature).

The collected data represent a variety of potentially nonlinear and covarying relationships requiring a suite of statistical tests to assess correlations and relationships across seasons, roof types and events. Non-parametric Mann–Whitney tests were used to determine the seasonal differences in meteorological antecedent descriptors. The differences in first-flush parameters between roof types were assessed using generalized ANOVA with a compound symmetry autocorrelation structure to account for the repeated measures of the same roofs (Zuur et al., 2009). Contrasts (pairwise comparisons) were assessed using the *emmeans* function of the R package emmeans (Lenth, 2020). Relationships between meteorological antecedent conditions and water quality response variables were tested using Spearman's correlation coefficients. Non-metric multidimensional scaling (NMDS) was used to qualitatively assess the water quality response of the different roofs based on the core response variables outlined above. All data were log-transformed prior to running ANOVA and NMDS analysis. Group (roof-type) centroids were calculated, and the mean distance from the centroid was used to assess response variability. All *P*-values were corrected for multiple testing using the Benjamini–Hochberg method (false discovery rate [FDR]) (Benjamini & Hochberg, 1995). All analyses were undertaken using R Version 3.6.2.

3 | RESULTS

3.1 | Meteorological conditions and storm antecedent conditions

The meteorological conditions during the study are presented in Figure 3. Air temperature was greater in August (Mann–Whitney $U = 65.3$, $P < 0.05$, +2.9 and +6.2°C compared to July and September, respectively). When compared to NOAA's climate data online for other years, these results followed the general trend for this region, with the exception that July was then the warmest summer month (within 1°C). The variability in the relative humidity decreased at the end of August (monthly mean of 69.0%) with generally higher values measured through September ($U = 42.4$, $P = 0.02$, between 15% and 19% more and monthly mean of 76.0%). There were no significant differences in the wind speed condition between months during the study period, with monthly mean from July to September, respectively being of 1.7, 1.5 and 1.6 m/s. The month of August was also slightly dryer (total precipitation of 142 mm, $U = 55.3$, $P = 0.01$) than July (150.9 mm) and September (150.1 mm).

Figure 4 presents the antecedent conditions for storm events. There was a decrease in the storm intensity in mid-August, with storm events having a longer duration towards the end of the period of observation. The mean duration for storm events 1–5 was 2.05 ± 1.71 h (mean ± SD), while for storms 6–15 was 6.18 ± 4.0 h. The 3-

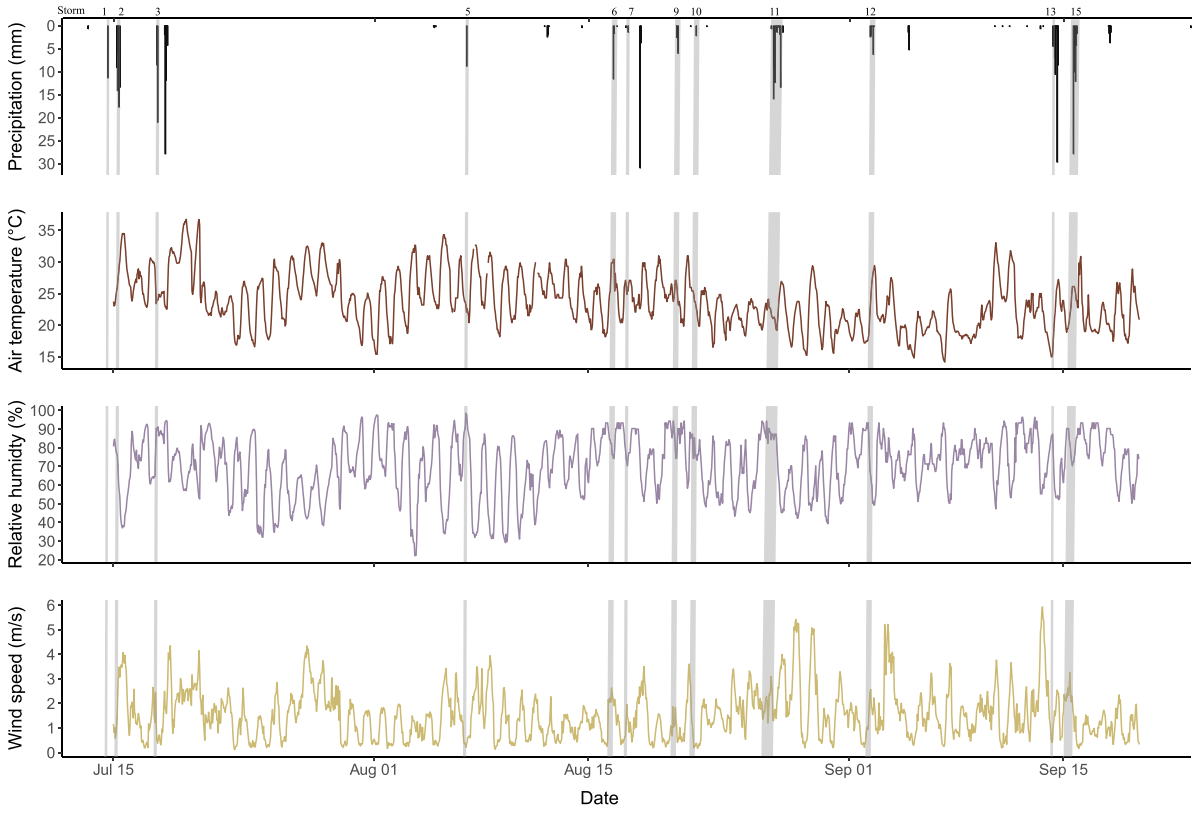

FIGURE 3 Meteorological conditions recorded during the study period. Grey bars denote storm period above threshold. Numbers indicate the storm number used for reference

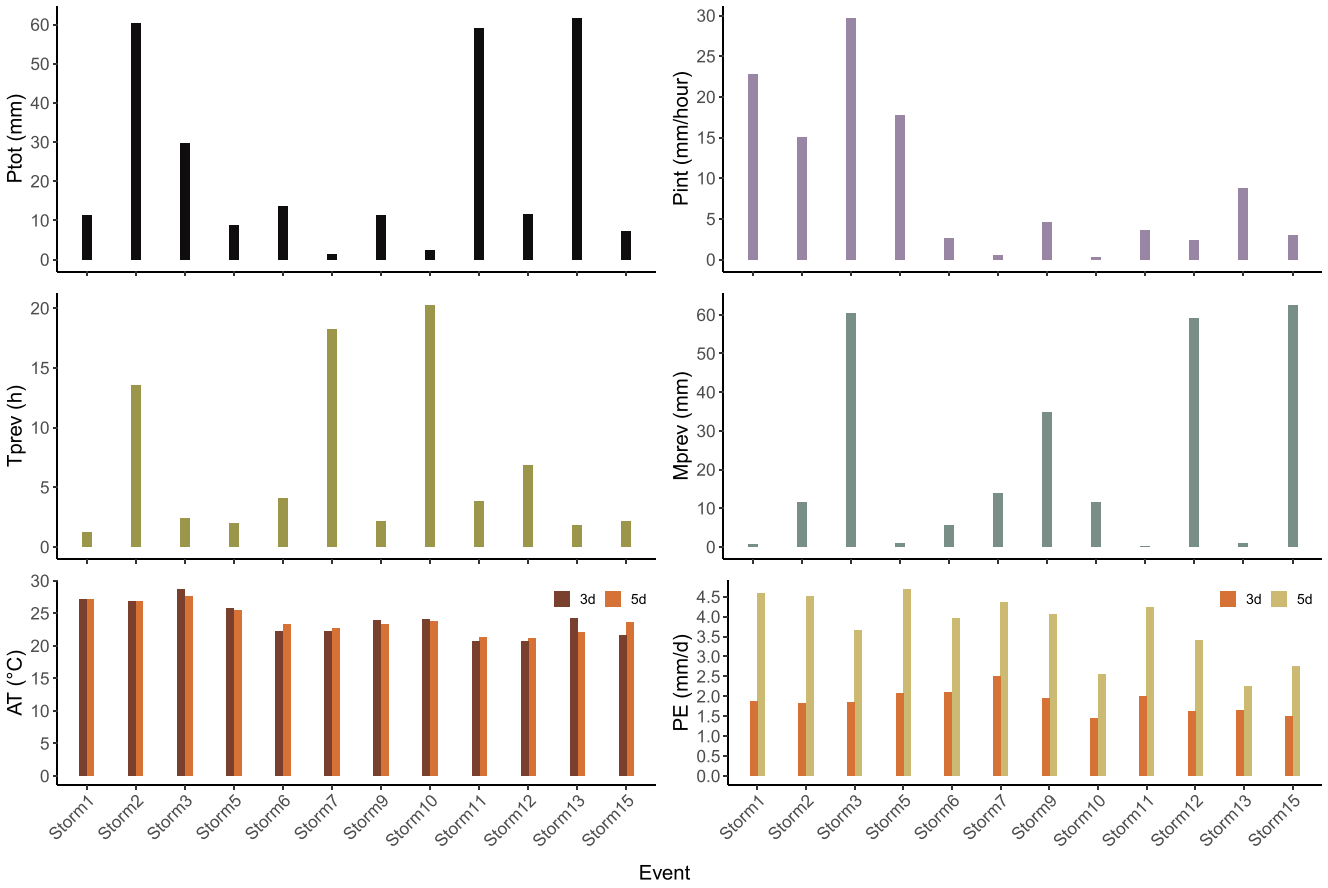

FIGURE 4 Antecedent conditions for each storm event, July to September 2019, where P_{tot} = sum of event precipitation, P_{int} = maximum precipitation intensity, T_{prev} = time (h) since previous event, M_{prev} = magnitude (total precipitation) of previous event, AT = moving average of air temperature and PE = sum of potential evapotranspiration

and 5-day air temperature moving average values were significantly lower for storms 11–15 ($U = 6.3$, $P = 0.005$), with respective mean values of 23.7 ± 1.8°C and 23.6 ± 21°C. In comparison, the mean values for the previous storms were 30.0 ± 2.7°C and 30.0 ± 1.6°C. The evapotranspiration 3- and 5-day moving average also decreasing after storm 9 ($U = 5.8$, $P = 0.007$), with mean values, respectively, decreasing from 2.0 ± 0.2 and 4.0 ± 0.4 mm/d to 1.7 ± 0.3 and 3.3 ± 0.8 mm/d, which correspond to the period with higher relative humidity values.

3.2 | Hydrological response

The roof response time, that is, the lag between storm event initiation and threshold exceedance, varied between roof types (Figure 5). The unmanaged GR generally displayed greater response time. However, for most of the storms of higher intensity that were preceded by a dryer period, the managed roof displayed a more delayed response than the unmanaged GR (e.g. Figure 4; Mprev, Storms 5, 11 and 13). With the exception of Storms 3 and 6, the non-vegetated roof always responded quicker than either GR. Although Storm 3 gained in intensity afterwards, both Storms 3 and 6 had an initial low-intensity phase, which could explain the delayed response in the non-vegetated roof as it is possible that the early small amount of rain evaporated from the non-vegetated roof due to a hotter surface (concrete surface).

3.3 | Water quality temporal dynamics

When considering general patterns of water quality across all roof types, seasonal dynamics were apparent. The electrical conductivity of roof runoff generally increased across the monitoring period, from 70.9 ± 23.7 µS/cm (mean ± SD) in July to 120.0 ± 38.3 µS/cm in September. Mean nitrate concentration did not follow EC and was higher in July and August than in September (Figure 6). DOC concentration decreased from 15.4 ± 8.1 mg/L in July to 7.9 ± 3.4 mg/L in September, while no clear temporal trend was apparent for DOC quality (SUVA and spectral slope; Figure 6). Mean water temperature of roof runoff decreased across the monitoring period from a high of 23.4 ± 0.8°C in July to 22.8 ± 1.2°C in September.

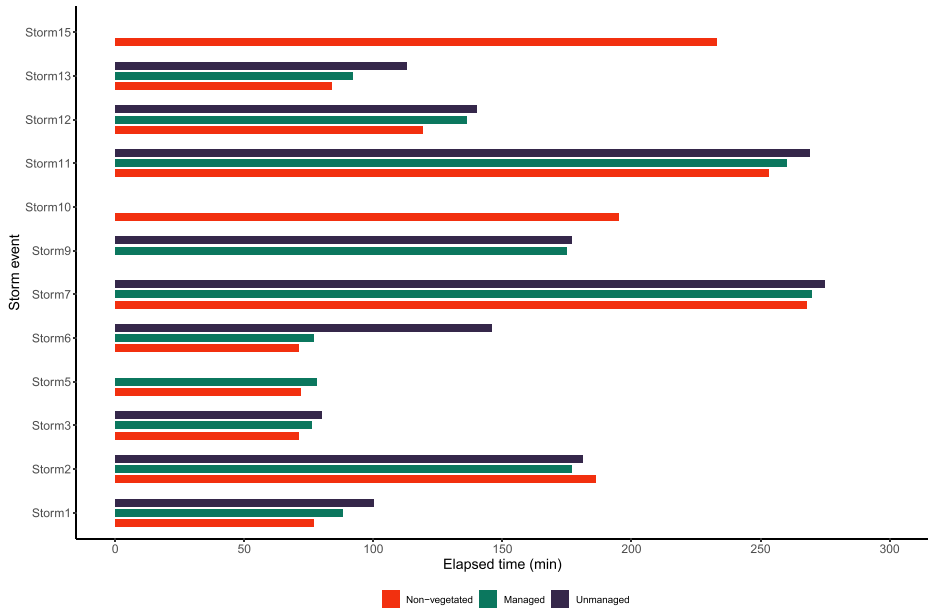

FIGURE 5 Roof response time between storm event initiation and threshold exceedance each roof

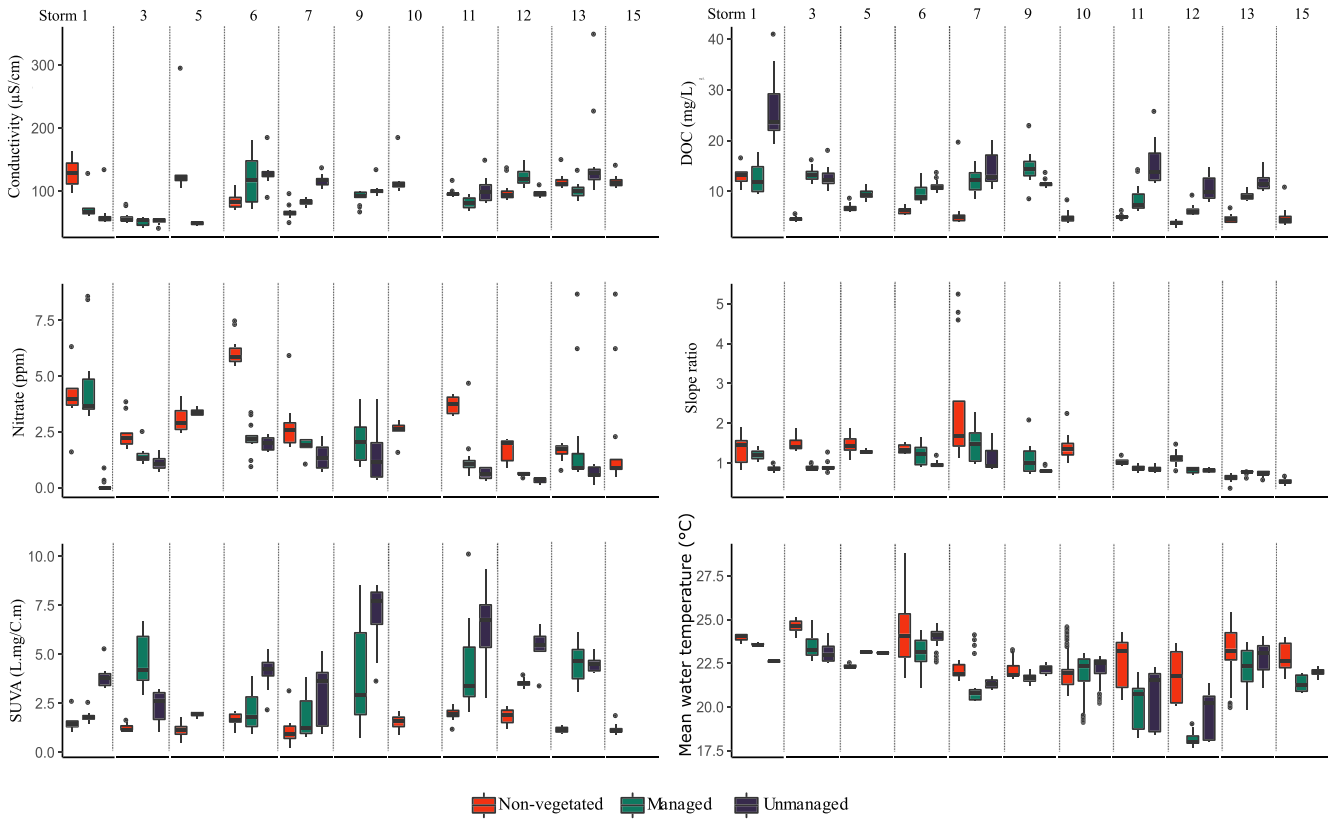

FIGURE 6 Water quality parameter boxplot showing the difference between the non-vegetated, managed and unmanaged roofs for each storm event. Lower values of spectral slope ratio indicate higher molecular weight DOM

3.4 | First-flush water quality response and meteorological drivers

Water quality of the first-flush stormwater runoff varied between the managed and unmanaged roofs (Table 2), with significant differences observed for DOM quality PC2. Both GR significantly differed from the non-vegated roof for DOC, DOM quality PC2 and SUVA. Interestingly, mean water temperature did not differ between the roof types. The first PCA axis (PC1) (69.9%; Figures 7 and S3 and Table S3) identified a strong gradient from highly aromatic DOM with higher SUVA

TABLE 2 Mean ± SE for key first-flush water quality variables (DOM quantity and quality, electrical conductivity, nitrate and water temperature)

Response variable (initial response)	Roof type			χ^2	*P*
	Non-vegetated	Managed GR	Unmanaged GR		
DOC (mg/L)	**6.3 ± 0.77 (a)**	**10.7 ± 0.94 (b)**	**17.1 ± 3.11 (b)**	**22.52**	**<0.001**
DOM quality PC1	**−2.96 ± 0.39 (a)**	**0.98 ± 0.46 (b)**	**2.47 ± 0.41 (c)**	**42.9**	**<0.001**
DOM quality PC2	−0.51 ± 0.59 (a)	0.51 ± 0.62 (a)	0.09 ± 0.34 (a)	0.84	0.66
SUVA (L.mg/C.m)	**3.82 ± 0.39 (a)**	**5.03 ± 0.27 (b)**	**5.50 ± 0.43 (b)**	**7.85**	**0.02**
Spectral slope ratio (SR)	1.27 ± 0.13 (a)	1.04 ± 0.08 (a)	0.89 ± 0.04 (a)	2.4	0.31
Nitrate (mg/L)	3.3 ± 0.54 (a)	2.2 ± 0.49 (a)	0.8 ± 0.30 (a)	2.23	0.33
Electrical conductivity (μS/cm)	111.3 ± 10.41 (a)	87.8 ± 8.4 (a)	109.1 ± 15.11 (a)	1.42	0.29
Mean water temp (°C)	21.9 ± 0.37 (a)	22.1 ± 0.34 (a)	22.1 ± 0.38 (a)	0.09	0.96

Notes: $\chi 2$ = chi-squared values based on a one-way ANOVA with a compound autocorrelation structure. Letters a, b and c denote significant differences based on a post hoc test. Bold text denotes significant differences with $P \leq 0.01$.

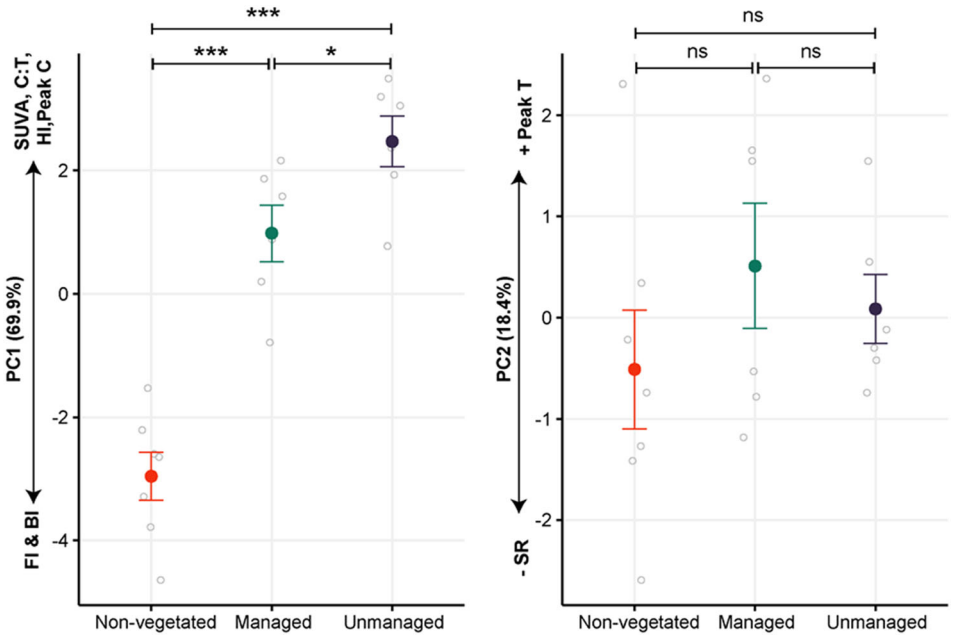

FIGURE 7 Dissolved organic matter quality PCA scores for (a) PC1 that was correlated with SUVA, Peak C:T ratio, HI and Peak C fluorescence intensity and (b) PC2 that was correlated with Peak T fluorescence intensity and spectral slope ratio. Circles represent mean scores for each roof type with error bars ± SE. Grey circles are scores for individual storms. See Figure S3 and Table S3 for ordination and correlations. *P*-values based on Fisher's LSD are also displayed not significant; **P* < 0.05, ***P* < 0.001

values and Peak C:T ratio (i.e. unmanaged GR) to fresher DOM associated with higher FI and spectral slope values (i.e. non-vegetated GR). Roof types were arrayed along PC1, with the non-vegetated roof displaying more negative values than both the managed GR (*z*-ratio = −4.59; *P* < 0.001) and the unmanaged GR (*z*-ratio = −6.31; *P* < 0.001). The unmanaged GR displaying more positive values than the managed GR (*z*-ratio = −1.69; *P* < 0.1). The second PCA axis (PC2) corresponded to the gradient of increasing tryptophan-like fluorescence and spectral slope ratio. No significant differences between roof types were apparent for PC2.

There were strong differences for DOC concentration, with the non-vegetated roof having a significantly lower mean DOC concentration compared to the managed GR (*z*-ratio = −2.17; *P* < 0.05) and unmanaged GR (*z*-ratio = −2.71; *P* < 0.01). However, while mean DOC was higher for the unmanaged roof compared to the managed roof (17.1 vs. 10.7 mg/L), this was not significant due to high variability between events (Table 2). There were no significant differences apparent for electrical conductivity across the three roofs, while nitrate values and mean water temperature were often higher for the non-vegetated roof but without differences between the vegetated roofs.

Non-metric dimensional scaling identified distinct structure in the first-flush dataset, with storm clustering by roof type along axis one (N-Ax1) (Figure 8). N-Ax1 was positively correlated with DOC ($\rho = 0.44$) and SUVA ($\rho = 0.51$) and negatively correlated with nitrate ($\rho = -0.95$) and spectral slope ($\rho = -0.78$). The roof types were significantly correlated with N-Ax1 (group centroid scores: non-vegetated −0.07, managed GR 0.01, unmanaged GR 0.09). For N-Ax2, a significant correlation was only apparent for electrical conductivity ($\rho = 0.86$).

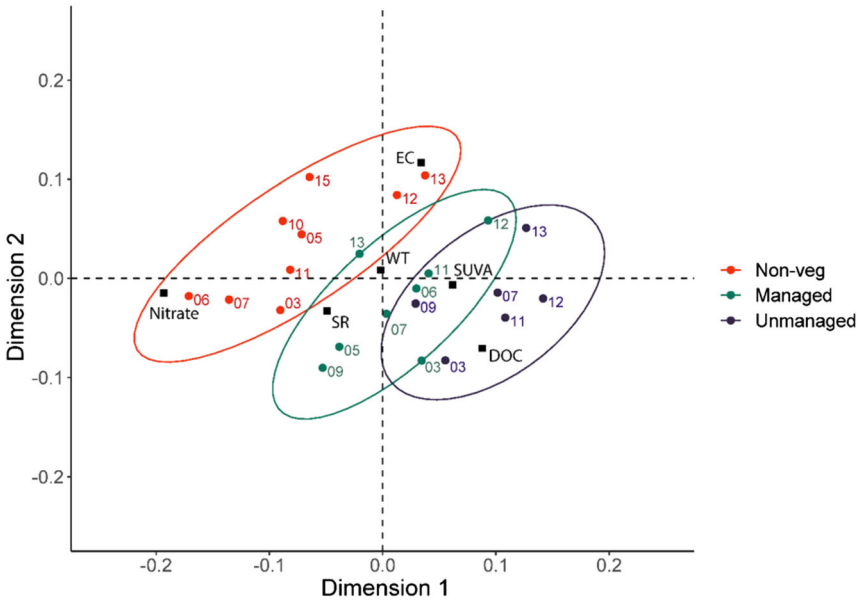

FIGURE 8 NMDS (stress = 0.12) of first-flush water quality variables. Squares represent water quality variable loadings, and filled circles individual storm events for each roof type. Roof type ellipses (95% CI) were fitted post hoc using a permutation procedure ($n = 999$) and were significantly related to the ordination ($R^2 = 0.4$, $P = 0.002$)

Limited relationships between DOM/nutrient first response and meteorological variables were found when assessing each roof type independently, with significant correlations only apparent for DOC, spectral slope and nitrate. For the unmanaged roof, DOC concentration was positively correlated with potential evapotranspiration and negatively correlated with the magnitude of the previous storm event (Table 3). For the non-vegetated roof, the spectral slope was negatively related to total precipitation, and nitrate was positively related to time since the previous event. For both the non-vegetated roof and managed GR, spectral slope was positively correlated with 5-day PE and 3-day AT (Table 3).

3.5 | Water temperature

The thermal response of each roof during a storm event was characterized by the time elapsed between the start of the storm and the time to reach the maximum water temperature change (Figure 9). The non-vegetated roof responded much quicker to rainfall than the vegetated roofs, except for Storms 3 and 6 for which the non-vegetated roof responded after the managed GR but still before the unmanaged GR. This delayed response seemed to be linked to the low intensity of the storm in the initial phase. The antecedent air temperature and evapotranspiration conditions were correlated with the thermal response metrics (except the rate of change) for the vegetated roofs, with the managed GR mainly responding more quickly when the antecedent air temperature and evapotranspiration were lower (Table 3). The mean (for all roof types) and maximum (for unmanaged GR) water temperatures were also negatively correlated with the storm intensity.

The difference in mean runoff temperature between the non-vegetated and vegetated roofs highlighted the capacity of GR to reduce thermal surge during rain events. The non-vegetated roof typically displayed warmer and more variable temperature than the GR (Figure 10). On two occasions (Storms 4 and 9), the GR released warmer water, which was especially true for the unmanaged roof. These two particular storms occurred following a succession of rain events and when the air temperature was hot (>30°C), suggesting a saturation of the soil and thermal build-up within the soil.

4 | DISCUSSION

We found that vegetated roofs can reduce the concentration of labile DOM, reduce the concentration of inorganic nitrogen concentration (i.e. NO_3) and mitigate thermal surges. Hence, GR, regardless of management regime, can be effective tools to mitigate urban stream syndrome. However, we identified that the responses were modulated by vegetation type and vegetation management. Indeed, the unmanaged GR showed lower nitrate concentration in runoff compared to the managed GR. Our results are also consistent with studies showing that rainfall is directly flushed from non-vegetated roofs without any processing time and that non-vegetated roofs release warmer water (Berndtsson et al., 2006; Cascone et al., 2018). Overall, the unmanaged GR was associated with lower nitrate and a less pronounced thermal surge relative to the managed GR. However, more DOC was exported, which is probably linked to the differences in the residence time. Additionally, under specific conditions, that is, warm air temperature and saturated soil, the thermal response of the GR after a storm can be a quick release of warmer water, similar to the behaviour of non-vegetated roofs. We found that the difference in the GR buffering capacity was mainly controlled by the vegetation assemblage on the roof and meteorological antecedent conditions: air temperature, evapotranspiration potential and the timing and magnitude of the previous rain event. Our study used fully functional and established GR, therefore providing pieces of evidence that are scalable for urban planning.

TABLE 3 Spearman's correlation coefficients to assess relationships between response variables and meteorological variables

Response	P_{int}			P_{tot}			AT_{5D}			PE_{5D}			T_{prev}			M_{prev}		
Variable	NV	M	UM	NV	M	UM	NV	M	UM	NV	M	UM	NV	M	UM	NV	M	UM
DOC												0.77						−0.78
Spectral slope ratio (SR)					−0.78		0.64	0.76		0.78								
Nitrate													0.81					
Mean water temperature	−0.76	−0.83	−0.59				0. 59	0.60			0.52							
Max water temperature			−0.52					0.61				0.52						
Min water temperature		0.57	0.58				0.55	0.66			0.52	0.51						
Maximum rate of change				0.54														

Notes: Correlations were calculated for each roof type independently (NV = non-vegetated, M = managed green roof and UM = unmanaged green roof). Note that only significant correlations are shown (significance level 0.05).

Abbreviations: AT_{5D}, 5-day moving average of air temperature; M_{prev}, magnitude (total precipitation) of previous event; PE_{5D}, 5-day sum of potential evapotranspiration; P_{int}, maximum precipitation intensity; P_{tot}, sum of event precipitation; T_{prev}, time (h) since previous event.

While some prior studies have assessed the impacts of GR on nutrient cycling and flux to the wider drainage network (Berndtsson, 2010; Mitchell et al., 2017; Speak et al., 2014), this study is the first to determine the composition of DOM rather than just a bulk measure (e.g. total DOC). During the first flush of stormwater, DOC concentration in runoff from the GR was an order of magnitude greater than from the non-vegetated roof. The absolute DOC concentrations for the GR in our study (11–17 mg/L) were lower than that observed for an experimental study in northern France (∼ 50 mg/L), but the relative differences between vegetated and non-vegetated roofs were comparable (Seidl et al., 2013). This consistent difference between GR and non-vegetated roofs reflects the increased biomass in GR, particularly carbon stocks in the soils, whereas organic matter exported from non-vegetated roofs reflects the mobilization of material deposited from the atmosphere (Buffam et al., 2016; Dunnett et al., 2008). Further, we found that DOC concentration in runoff from the unmanaged GR was generally higher than for the managed roof, likely reflecting differences in soil organic content associated with vegetation type and density (Livesley et al., 2016). Additionally, the longer residence time of the unmanaged roof probably also leads to greater carbon leaching.

Carbon quality also differed strongly across the roof types, with the non-vegetated roof displaying a DOM signal comparable to that of road runoff/impervious surface (Khamis et al., 2018; McElmurry et al., 2014). The low molecular weight (high SR), low aromaticity and high Peak T and FI values (Figure S2) suggested that the DOM from the non-vegetated roof was fresher and labile and therefore may be rapidly processed in receiving waters. The $SUVA_{254}$ was strongly elevated for the GR relative to the non-vegetated roof, indicating DOM of high aromaticity (comparable to forest runoff) transported from GR to the drainage network (McElmurry et al., 2014; Peacock et al., 2015). Differences between the managed and unmanaged roofs were less pronounced, but suggested DOM was slightly less aromatic and less recalcitrant for the managed GR. The difference in DOM quality has important management implications. While a more natural DOM signal is desirable (e.g. reduce oxygen demand in urban rivers), there may be downstream consequences such as changes in community respiration, water clarity/colour and an elevated risk of carcinogenic by-product formation during water treatment (Ritson et al., 2014).

Although studies on experimental plots have previously highlighted that GR can leach phosphorus, organic carbon, nitrogen and metals during rain events (e.g. Buffam & Mitchell, 2015), little is still known on the leaching behaviour of full-scale functional GR. We did not observe nutrient leaching, suggesting that nutrient uptake is more efficient on well-established full-scale roofs. We also found lower nitrate concentration in runoff from the vegetated GR, especially for the unmanaged GR, which can be explained by its slower hydrological response (time response) and higher evapotranspiration rates. Indeed, our results showed that air temperature, evapotranspiration antecedent conditions and the time since—and magnitude of—the previous rain event are important drivers of the GR ecohydrological behaviours. Although not measured here, fully

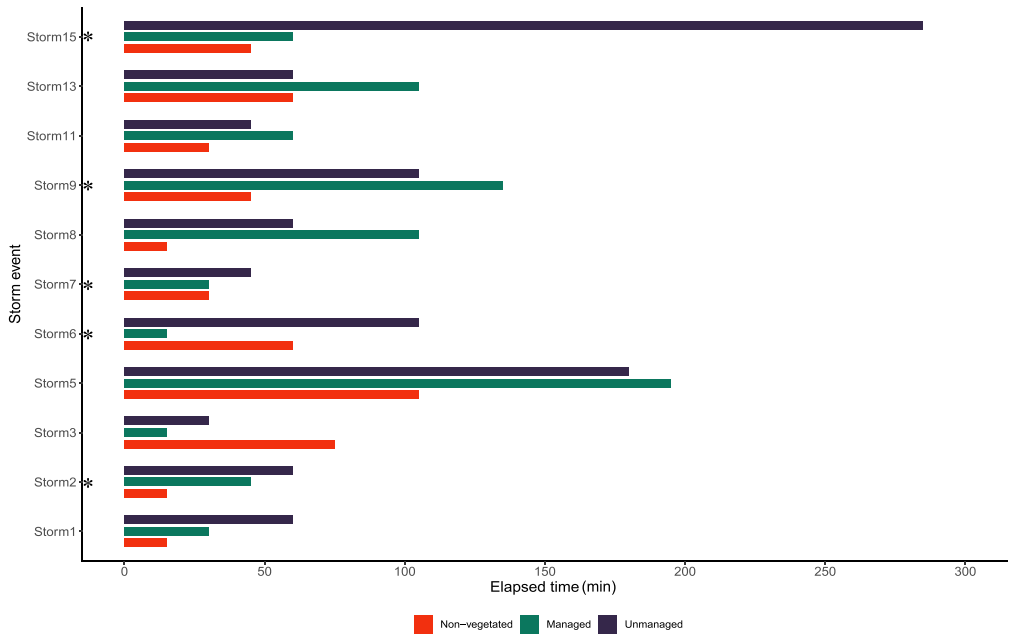

FIGURE 9 Elapsed time between the start of the rainfall event and the maximum thermal change (either max or min) on each roof. Asterisk indicates the storms for which the water temperature decreased after the start of the rain

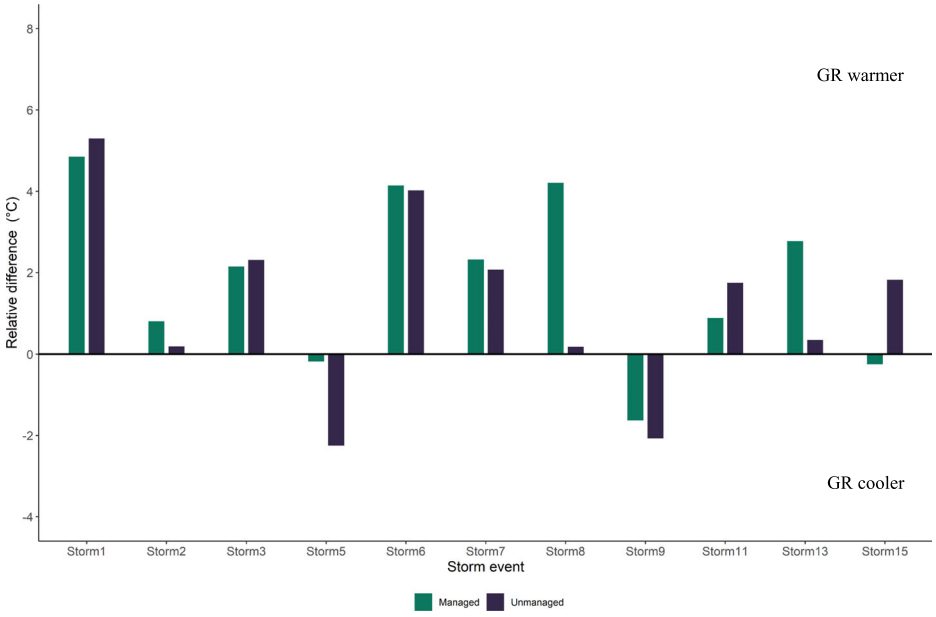

FIGURE 10 Relative temperature differences between the non-vegetated and vegetated roofs ($T_{non\text{-}veg} - T_{GR}$) for each storm event

functional vegetated roofs should also have an established microbial community, leading to increased nutrient processing (Mitchell et al., 2018). Nutrient processing, as our results suggested, is also directly influenced by the evapotranspiration rates, which drive the roof buffering capacity and processing time, as well as the temperature conditions, which modulate microbial activity, mineralization, weathering and desorption rates. Finding the ideal evaporation rates to maximize the nutrients processing linked with roof vegetation management can help improve GR design to more efficiently target the reduction of inorganic nitrogen fluxes.

Thermal effects of GR on runoff are rarely assessed, as most studies focus on building cooling for energy savings (Eksi et al., 2017; Imran et al., 2018; Sharma et al., 2016) or mitigating UHI (Cao et al., 2019; Stamenković et al., 2018). We found that both vegetated roofs released slightly cooler water when compared to a non-vegetated roof. They also displayed a delayed thermal response due

to their longer response times, with a more significant effect observed in the unmanaged GR. However, we also found that GR can induce warmer runoff temperatures when the soil is already saturated with warm water, which is most likely due to thermal build-up in the vegetated GR. Indeed, heat exchanges on concrete surfaces are typically more dynamics (faster warming and cooling rates) compared to surfaces with vegetation, where evapotranspiration fluxes strongly influence heat exchange (Timm et al., 2020). Therefore, specific conditions, such as warm air temperatures combined with soil saturation, leading to longer residence time, allowed for thermal build-up to happen. These findings highlighted the need to optimize evapotranspiration and drainage in the GR design to avoid the production of thermal surges. It is important to acknowledge that even if thermal surges do not reach detrimental values for cold-water species, they still contribute to the overall thermal degradation of urban streams and ultimately negatively impact ecological functioning. Therefore, it is important to improve understanding of the relationship between the roof retention time and the thermal response. To our knowledge, this study is the first to provide information on functional GR thermal behaviour for a range of rain events, which is important for guiding management efforts focused on reducing thermal pollution of urban waters.

GR management strategies can explain the observed differences in buffering capacity and initial response. The amount of water runoff and delay in the peak flow are mainly controlled by the vegetation type and the type of substratum (Liu, Feng, et al., 2019; Nagase & Dunnett, 2012; Wong & Jim, 2014). As plants have different capacities for water interception, retention and transpiration, the types of plants are a strong determinant of GR runoff mitigation capacity. Moreover, dense fibrous roots capture less runoff because they reduce the volume of the medium available to retain water (MacIvor & Lundholm, 2011). Some studies have highlighted that taller plants, such as graminoids, which dominate the unmanaged GR, have a greater interception potential compared to low-growing or mat-forming plants due to a greater exposed surface area and higher evapotranspiration rates (Dunnett et al., 2008; MacIvor & Lundholm, 2011). Therefore, the choice of plants and their above- and underground structural architecture, as well as the community composition, strongly influence GR stormwater mitigation (Butler & Orians, 2011; Cook-Patton & Bauerle, 2012; Lundholm et al., 2010). These observations are consistent with our results, as we found that the unmanaged GR, which has a greater area colonized by plants, with taller plants (Figure 2), was associated with lower nitrate concentration and thermal surges in runoff.

5 | CONLUSION AND IMPLICATIONS

Overall, our results provide insightful information between the GR response behaviour and vegetation management, showing that GR with more diverse and dense vegetation may have better mitigation potential of water quality degradation. They also highlighted the GR potential to reduce DOC and nitrate concentration and export less humic-like DOM signal, as well as thermal surges. GR can provide many benefits to offset the negative impacts of urban development. Still, the design of GR for regional resilience requires a deeper understanding of GR ecosystems themselves, including vegetation type and management, microbial and invertebrate diversity and activity and the role of the substratum and drainage conditions in GR ecosystem structure and function. Our study highlights the importance of understanding processes and outcomes using fully functional, well-established GR.

Due to the limited understanding of the overall effects of GR on surrounding ecosystems, their potential for large-scale implementation as a tool to mitigate impaired urban water quality is still uncertain. The seasonality and long-term stability (years to decades) of GR have been overlooked so far. There is a strong need to assess the impacts of these two determinant factors that directly influence the GR response times of physico-chemical and biological processes. Indeed, reaction rates are strongly controlled by seasonal patterns such as the plant growing season and age and the ambient temperature conditions, as well as the storm frequency and magnitude (dry vs. wet seasons). Understanding how these factors influence the optimal drainage time is crucial to allow for beneficial nutrient processing without retaining too much water, which will subsequently cause unwanted thermal surges. GR should therefore be seen as functional ecosystems, and future studies should fully integrate the different characteristics of GR, including their shallow soil habitats and the associated invertebrate and microbial biodiversity, which affects soil structure, hydrologic response and availability of organic carbon and nutrients. Indeed, understanding the synergetic interactions between these components over multiple growing seasons, as the overall optimal design may not be optimal for any given season, and at a relevant scale for management is needed to unravel the complexity of GR behaviour. This new knowledge generated would support design strategies allowing for a more efficient offset of the impacts of urbanization and climate change on terrestrial and aquatic urban ecosystems and contribute to maximizing the value of current investments to integrate GR into urban design.

ACKNOWLEDGEMENTS

The authors are thankful to the Chicago Botanic Garden for allowing us to use and access their green roof infrastructures. We also thank Vincent Huang, Jordan Gurneau and Maya Weiss for their field and laboratory work assistance. The main funding for this project came from European Union's Horizon 2020 Research and Innovation Programme under the Marie Sklodowska-Curie Grant Agreement Number 34317 (HiFreq). This work was also supported by U.S. National Science Foundation award number CBET-1848683.

CONFLICTS OF INTEREST

The authors declare no conflict of interest.

DATA AVAILABILITY STATEMENT

The authors confirm that the data supporting the findings of this study are available in the Supporting Information.

ORCID

Valerie Ouellet https://orcid.org/0000-0001-7410-1857
Kieran Khamis https://orcid.org/0000-0002-5203-3221
Danny Croghan https://orcid.org/0000-0003-1857-2528
Collin B. Phillips https://orcid.org/0000-0001-9950-2497
Aaron I. Packman https://orcid.org/0000-0003-3172-4549
William M. Miller https://orcid.org/0000-0003-0750-6314
David M. Hannah https://orcid.org/0000-0003-1714-1240
Stefan Krause https://orcid.org/0000-0003-2521-2248

REFERENCES

Baker, A. (2001). Fluorescence excitation-emission matrix characterization of some sewage-impacted rivers. *Environmental Science and Technology*, *35*(5), 948–953. https://doi.org/10.1021/es000177t

Beck, D., Johnson, G., & Spolek, G. (2011). Amending greenroof soil with biochar to affect runoff water quantity and quality. *Environmental Pollution*, *159*(8-9), 2111–2118.

Beecham, S., & Razzaghmanesh, M. (2015). Water quality and quantity investigation of green roofs in a dry climate. *Water Research*, *70*, 370–384. https://doi.org/10.1016/j.watres.2014.12.015

Benjamini, Y., & Hochberg, Y. (1995). Controlling the false discovery rate: A practical and powerful approach to multiple testing. *Journal of the Royal Statistical Society*, *57*(1), 289–300. https://doi.org/10.1111/j.2517-6161.1995.tb02031.x

Berndtsson, J. C. (2010). Green roof performance towards management of runoff water quantity and quality: A review. *Ecological Engineering*, *36*(4), 351–360. https://doi.org/10.1016/j.ecoleng.2009.12.014

Berndtsson, J. C., Bengtsson, L., & Jinno, K. (2008). First flush effect from vegetated roofs during simulated rain events. *Hydrology Research*, *39*(3), 171–179. https://doi.org/10.2166/nh.2008.044

Berndtsson, J. C., Emilsson, T., & Bengtsson, L. (2006). The influence of extensive vegetated roofs on runoff water quality. *Science of the Total Environment*, *355*(1–3), 48–63. https://doi.org/10.1016/j.scitotenv.2005.02.035

Buffam, I., & Mitchell, M. E. (2015). Nutrient cycling in green roof ecosystems. In R. Sutton (Ed.), *Green roof ecosystems* (Vol. 223). Ecological Studies (Analysis and Synthesis). (pp. 107–137). Springer.

Buffam, I., Mitchell, M. E., & Durtsche, R. D. (2016). Environmental drivers of seasonal variation in green roof runoff water quality. *Ecological Engineering*, *91*, 506–514. https://doi.org/10.1016/j.ecoleng.2016.02.044

Butler, C., & Orians, C. M. (2011). Sedum cools soil and can improve neighboring plant performance during water deficit on a green roof. *Ecological Engineering*, *37*(11), 1796–1803. https://doi.org/10.1016/j.ecoleng.2011.06.025

Cao, J. J., Hu, S., Dong, Q., Liu, L. J., & Wang, Z. L. (2019). Green roof cooling contributed by plant species with different photosynthetic strategies. *Energy and Buildings*, *195*, 45–50. https://doi.org/10.1016/j.enbuild.2019.04.046

Cascone, S., Catania, F., Gagliano, A., & Sciuto, G. (2018). A comprehensive study on green roof performance for retrofitting existing buildings. *Building and Environment*, *136*, 227–239. https://doi.org/10.1016/j.buildenv.2018.03.052

Cipolla, S. S., Maglionico, M., & Stojkov, I. (2016). A long-term hydrological modelling of an extensive green roof by means of SWMM. *Ecological Engineering*, *95*, 876–887. https://doi.org/10.1016/j.ecoleng.2016.07.009

Coker, M. E., Bond, N. R., Chee, Y. E., & Walsh, C. J. (2018). Alternatives to biodiversity offsets for mitigating the effects of urbanization on stream ecosystems. *Conservation Biology*, *32*(4), 789–797. https://doi.org/10.1111/cobi.13057

Colegrave, N., & Ruxton, G. D. (2018). Using biological insight and pragmatism when thinking about Pseudoreplication. *Trends in Ecology & Evolution*, *33*(1), 28–35.

Cook-Patton, S. C., & Bauerle, T. L. (2012). Potential benefits of plant diversity on vegetated roofs: A literature review. *Journal of Environmental Management*, *106*, 85–92. https://doi.org/10.1016/j.jenvman.2012.04.003

Croghan, D., Van Loon, A. F., Sadler, J. P., Bradley, C., & Hannah, D. M. (2019). Prediction of river temperature surges is dependent on precipitation method. *Hydrological Processes*, *33*(1), 144–159. https://doi.org/10.1002/hyp.13317

D'Amour, C. B., Reitsma, F., Baiocchi, G., Barthel, S., Güneralp, B., Erb, K. H., Haberl, H., Creutzig, F., & Seto, K. C. (2017). Future urban land expansion and implications for global croplands. *Proceedings of the National Academy of Sciences of the United States of America*, *114*(34), 8939–8944. https://doi.org/10.1073/pnas.1606036114

Davies, G. M., & Gray, A. (2015). Do not let spurious accusations of pseudoreplication limit our ability to learn from natural experiments (and other messy kinds of ecological monitoring). *Ecology and Evolution*, *5*(22), 5295–5304.

Deilami, K., Kamruzzaman, M., & Liu, Y. (2018). Urban heat island effect: A systematic review of spatio-temporal factors, data, methods, and mitigation measures. *International Journal of Applied Earth Observation and Geoinformation*, *67*, 30–42. https://doi.org/10.1016/j.jag.2017.12.009

Dunnett, N., Nagase, A., Booth, R., & Grime, P. (2008). Influence of vegetation composition on runoff in two simulated green roof experiments. *Urban Ecosystem*, *11*(4), 385–398. https://doi.org/10.1007/s11252-008-0064-9

Dusza, Y., Barot, S., Kraepiel, Y., Lata, J. C., Abbadie, L., & Raynaud, X. (2017). Multifunctionality is affected by interactions between green roof plant species, substrate depth, and substrate type. *Ecology and Evolution*, *7*(7), 2357–2369. https://doi.org/10.1002/ece3.2691

Eksi, M., Rowe, D. B., Wichman, I. S., & Andresen, J. A. (2017). Effect of substrate depth, vegetation type, and season on green roof thermal properties. *Energy and Buildings*, *145*, 174–187. https://doi.org/10.1016/j.enbuild.2017.04.017

Frazer, L. (2005). Paving paradise: The peril of impervious surface. *Environmental Health Perspectives*, *113*, 457–462. https://doi.org/10.1289/ehp.113-a456

Guo, Y., Gasparrini, A., Li, S., Sera, F., Vicedo-Cabrera, A. M., de Sousa Zanotti Stagliorio Coelho, M., … Tong, S. (2018). Quantifying excess deaths related to heatwaves under climate change scenarios: A multicountry time series modelling study. *PLoS Medicine*, *15*(7), 1–17. https://doi.org/10.1371/journal.pmed.1002629

Hansen, A., Kraus, T. E. C., Pellerin, B., Fleck, J., Downing, B. D., & Bergamaschi, B. (2016). Optical properties of dissolved organic matter (DOM): Effects of biological and photolytic degradation. *Limnology and Oceanography*, *61*(3), 1015–1032. https://doi.org/10.1002/lno.10270

Hashemi, S. S. G., Mahmud, H. B., & Ashraf, M. A. (2015). Performance of green roofs with respect to water quality and reduction of energy consumption in tropics: A review. *Renewable and Sustainable Energy Reviews*, *52*, 669–679. https://doi.org/10.1016/j.rser.2015.07.163

Hawke, R. (2015). An evaluation study of plants for use on green roofs. In Plant Evaluation Notes, Chicago Botanic Garden, Chicago.

He, X., Wang, J., Feng, J., Yan, Z., Miao, S., Zhang, Y., & Xia, J. (2020). Observational and modeling study of interactions between urban heat island and heatwave in Beijing. *Journal of Cleaner Production*, *247*, 119169. https://doi.org/10.1016/j.jclepro.2019.119169

Helms, J. R., Stubbins, A., Ritchie, J. D., Minor, E. C., Kieber, D. J., & Mopper, K. (2008). Absorption spectral slopes and slope ratios as indicators of molecular weight, source, and photobleaching of chromophoric dissolved organic matter. *Limnology and Oceanography*, *53*(3), 955–969. https://doi.org/10.4319/lo.2008.53.3.0955

Hoch, J. M. K., Rhodes, M. E., Shek, K. L., Dinwiddie, D., Hiebert, T. C., Gill, A. S., Salazar Estrada, A. E., Griffin, K. L., Palmer, M. I., &

McGuire, K. L. (2019). Soil microbial assemblages are linked to plant community composition and contribute to ecosystem services on urban green roofs. *Frontiers in Ecology and Evolution*, *7*, 1–14. https://doi.org/10.3389/fevo.2019.00198

Hu, M., Zhang, X., Li, Y., Yang, H., & Tanaka, K. (2019). Flood mitigation performance of low impact development technologies under different storms for retrofitting an urbanized area. *Journal of Cleaner Production*, *222*, 373–380. https://doi.org/10.1016/j.jclepro.2019.03.044

Husson, F., Josse, J., Le, S., & Mazet, J. (2014). FactoMineR - R package. http://factominer.free.fr

Imran, H. M., Kala, J., Ng, A. W. M., & Muthukumaran, S. (2018). Effectiveness of green and cool roofs in mitigating urban heat island effects during a heatwave event in the city of Melbourne in southeast Australia. *Journal of Cleaner Production*, *197*, 393–405. https://doi.org/10.1016/j.jclepro.2018.06.179

Ketabchy, M., Sample, D. J., Wynn-Thompson, T., & Nayeb Yazdi, M. (2018). Thermal evaluation of urbanization using a hybrid approach. *Journal of Environmental Management*, *226*, 457–475. https://doi.org/10.1016/j.jenvman.2018.08.016

Khamis, K., Bradley, B., & Hannah, D. M. (2018). Understanding dissolved organic matter dynamics in urban catchments: Insights from in situfluorescence sensor technology. *WIREs Water*, *5*, 1–14.

Lata, J. C., Dusza, Y., Abbadie, L., Barot, S., Carmignac, D., Gendreau, E., Kraepiel, Y., Mériguet, J., Motard, E., & Raynaud, X. (2018). Role of substrate properties in the provision of multifunctional green roof ecosystem services. *Applied Soil Ecology*, *123*, 464–468. https://doi.org/10.1016/j.apsoil.2017.09.012

Lawaetz, A. J., & Stedmon, C. A. (2009). Fluorescence intensity calibration using the Raman scatter peak of water. *Applied Spectroscoy*, *63*(8), 936–940.

Lenth, R. (2020). emmeans: Estimated marginal means, aka least-squares means (version 1.4. 2) [R package].

Liu, W., Feng, Q., Chen, W., Wei, W., & Deo, R. C. (2019). The influence of structural factors on stormwater runoff retention of extensive green roofs: New evidence from scale-based models and real experiments. *Journal of Hydrology*, *569*, 230–238. https://doi.org/10.1016/j.jhydrol.2018.11.066

Liu, W., Wei, W., Chen, W., Deo, R. C., Si, J., Xi, H., … Feng, Q. (2019). The impacts of substrate and vegetation on stormwater runoff quality from extensive green roofs. *Journal of Hydrology*, *576*, 575–582. https://doi.org/10.1016/j.jhydrol.2019.06.061

Livesley, S. J., Ossola, A., Threlfall, C. G., Hahs, A. K., & Williams, N. S. G. (2016). Soil carbon and carbon/nitrogen ratio change under tree canopy, tall grass, and turf grass areas of urban green space. *Journal of Environmental Quality*, *45*(1), 215–223. https://doi.org/10.2134/jeq2015.03.0121

Loiola, C., Wellington, M., & Pimentel da Silva, L. (2019). Hydrological performance of modular-tray green roof system for increasing the resilience of mega0cities to climate change. *Journal of Hydrology*, *573*, 1057–1066.

Lundholm, J., MacIvor, J. S., MacDougall, Z., & Ranalli, M. (2010). Plant species and functional group combinations affect green roof ecosystem functions. *PLoS ONE*, *5*(3), 1–11. https://doi.org/10.1371/journal.pone.0009677

MacIvor, J. S., & Lundholm, J. (2011). Performance evaluation of native plants suited to extensive green roof conditions in a maritime climate. *Ecological Engineering*, *37*(3), 407–417. https://doi.org/10.1016/j.ecoleng.2010.10.004

McElmurry, S. P., Long, D. T., & Voice, T. C. (2014). Stormwater dissolved organic matter: Influence of land cover and environmental factors. *Environmental Science and Technology*, *48*(1), 45–53. https://doi.org/10.1021/es402664t

Mentens, J., Raes, D., & Hermy, M. (2006). Green roofs as a tool for solving the rainwater runoff problem in the urbanized 21st century? *Landscape and Urban Planning*, *77*(3), 217–226. https://doi.org/10.1016/j.landurbplan.2005.02.010

Mitchell, M. E., Hamilton, T. L., Uebel-Niemeier, C., Hopfensperger, K. N., & Buffam, I. (2018). Nitrogen cycling players and processes in green roof ecosystems. *Applied Soil Ecology*, *132*, 114–125. https://doi.org/10.1016/j.apsoil.2018.08.007

Mitchell, M. E., Matter, S. F., Durtsche, R. D., & Buffam, I. (2017). Elevated phosphorus: Dynamics during four years of green roof development. *Urban Ecosystem*, *20*(5), 1121–1133. https://doi.org/10.1007/s11252-017-0664-3

Mohajerani, A., Bakaric, J., & Jeffrey-Bailey, T. (2017). The urban heat island effect, its causes, and mitigation, with reference to the thermal properties of asphalt concrete. *Journal of Environmental Management*, *197*, 522–538. https://doi.org/10.1016/j.jenvman.2017.03.095

Nagase, A., & Dunnett, N. (2012). Amount of water runoff from different vegetation types on extensive green roofs: Effects of plant species, diversity and plant structure. *Landscape and Urban Planning*, *104*(3–4), 356–363. https://doi.org/10.1016/j.landurbplan.2011.11.001

Nelson, K. C., & Palmer, M. A. (2007). Stream temperature surges under urbanization and climate change: Data, models, and responses. *Journal of the American Water Resources Association*, *43*(2), 440–452. https://doi.org/10.1111/j.1752-1688.2007.00034.x

NOAA. (2020). Climate data online. https://www.ncdc.noaa.gov/cdo-web/#t=secondTabLink

Peacock, M., Freeman, C., Gauci, V., Lebron, I., & Evans, C. D. (2015). Investigations of freezing and cold storage for the analysis of peatland dissolved organic carbon (DOC) and absorbance properties. *Environmental Science Processes & Impacts*, *17*, 1290–1301.

Pour, S. H., Wahab, A. K. A., Shahid, S., Asaduzzaman, M., & Dewan, A. (2020). Low impact development techniques to mitigate the impacts of climate-change-induced urban floods: Current trends, issues and challenges. *Sustainable Cities and Society*, *62*, 102373. https://doi.org/10.1016/j.scs.2020.102373

Ritson, J. P., Graham, N. J. D., Templeton, M. R., Clark, J. M., Gough, R., & Freeman, C. (2014). The impact of climate change on the treatability of dissolved organic matter (DOM) in upland water supplies: A UK perspective. *Science of the Total Environment*, *473–474*, 714–730. https://doi.org/10.1016/j.scitotenv.2013.12.095

Santamouris, M. (2014). On the energy impact of urban heat island and global warming on buildings. *Energy and Buildings*, *82*, 100–113. https://doi.org/10.1016/j.enbuild.2014.07.022

Seidl, M., Gromaire, M. C., Saad, M., & De Gouvello, B. (2013). Effect of substrate depth and rain-event history on the pollutant abatement of green roofs. *Environmental Pollution (Barking, Essex: 1987)*, *183*, 195–203. https://doi.org/10.1016/j.envpol.2013.05.026

Seto, K. C., Güneralp, B., & Hutyra, L. R. (2012). Global forecasts of urban expansion to 2030 and direct impacts on biodiversity and carbon pools. *Proceedings of the National Academy of Sciences*, *109*(40), 16083–16088. https://doi.org/10.1073/PNAS.1211658109

Shafique, M., Kim, R., & Rafiq, M. (2018). Green roof benefits, opportunities and challenges – A review. *Renewable and Sustainable Energy Reviews*, *90*, 757–773. https://doi.org/10.1016/j.rser.2018.04.006

Sharma, A., Conry, P., Fernando, H. J. S., Hamlet, A. F., Hellmann, J. J., & Chen, F. (2016). Green and cool roofs to mitigate urban heat island effects in the Chicago metropolitan area: Evaluation with a regional climate model. *Environmental Research Letters*, *11*(6), 1–15. https://doi.org/10.1088/1748-9326/11/6/064004

Sohn, W., Kim, J. H., & Li, M. H. (2017). Low-impact development for impervious surface connectivity mitigation: Assessment of directly connected impervious areas (DCIAs). *Journal of Environmental Planning and Management*, *60*(10), 1871–1889. https://doi.org/10.1080/09640568.2016.1264929

Somers, K. a., Bernhardt, E. S., Grace, J. B., Hassett, B. A., Sudduth, E. B., Wang, S., & Urban, D. L. (2013). Streams in the urban heat island:

Spatial and temporal variability in temperature. *Freshwater Science*, *32*(1), 309–326. https://doi.org/10.1899/12-046.1

Speak, A. F., Rothwell, J. J., Lindley, S. J., & Smith, C. L. (2014). Metal and nutrient dynamics on an aged intensive green roof. *Environmental Pollution*, *184*(3), 33–43. https://doi.org/10.1016/j.envpol.2013.08.017

Stamenković, M. G., Miletić, M. J., Kosanović, S. M., Vučković, G. D., & Glišović, S. M. (2018). Impact of a building shape factor on space cooling energy performance in the green roof concept implementation. *Thermal Science*, *22*(1), 687–698. https://doi.org/10.2298/TSCI170425205S

Thuring, C. E., & Dunnett, N. P. (2019). Persistence, loss and gain: Characterising mature green roof vegetation by functional composition. *Landscape and Urban Planning*, *185*, 228–236. https://doi.org/10.1016/j.landurbplan.2018.10.026

Timm, A., Ouellet, V., & Daniels, M. (2020). Swimming through the urban heat island: Can thermal mitigation practices reduce the stress? *River Research and Applications*, *36*(10), 1973–1984. https://doi.org/10.1002/rra.3732

United Nations, Department of Economic and Social Affairs, Population Division. (2019). World population prospects 2019: Data booklet (ST/ESA/SER.A/424). https://population.un.org/wpp/Publications/Files/WPP2019_DataBooklet.pdf

Ward, K., Lauf, S., Kleinschmit, B., & Endlicher, W. (2016). Heat waves and urban heat islands in Europe: A review of relevant drivers. *Science of the Total Environment*, *569–570*, 527–539. https://doi.org/10.1016/j.scitotenv.2016.06.119

Weishaar, J. L., Aiken, G. R., Bergamaschi, B. A., Fram, M. S., Fujii, R., & Mopper, K. (2003). Evaluation of specific ultraviolet absorbance as an indicator of the chemical composition and reactivity of dissolved organic carbon. *Enivironmental Science Technology*, *37*(20), 4702–4708. https://doi.org/10.1021/es030360x

Whittinghill, L. J., Hsueh, D., Culligan, P., & Plunz, R. (2016). Stormwater performance of a full scale rooftop farm: Runoff water quality. *Ecological Engineering*, *91*, 195–206. https://doi.org/10.1016/j.ecoleng.2016.01.047

Wong, G. K. L., & Jim, C. Y. (2014). Quantitative hydrologic performance of extensive green roof under humid-tropical rainfall regime. *Ecological Engineering*, *70*, 366–378. https://doi.org/10.1016/j.ecoleng.2014.06.025

Zhang, Z., Szota, C., Fletcher, T. D., Williams, N. S. G., & Farrell, C. (2019). Green roof storage capacity can be more important than evapotranspiration for retention performance. *Journal of Environmental Management*, *232*, 404–412. https://doi.org/10.1016/j.jenvman.2018.11.070

Zuur, A., Ieno, E. N., Walker, N., Saveliev, A. A., & Smith, G. M. (2009). *Mixed effects models and extensions in ecology with R*. Springer Science & Business Media.

SUPPORTING INFORMATION

Additional supporting information may be found online in the Supporting Information section at the end of this article.

How to cite this article: Ouellet, V., Khamis, K., Croghan, D., Hernandez Gonzalez, L. M., Rivera, V. A., Phillips, C. B., Packman, A. I., Miller, W. M., Hawke, R. G., Hannah, D. M., & Krause, S. (2021). Green roof vegetation management alters potential for water quality and temperature mitigation. *Ecohydrology*, e2321. https://doi.org/10.1002/eco.2321